IEEE Access
Multidisciplinary | Rapid Review | Open Access Journal

Received April 15, 2019, accepted May 8, 2019, date of publication May 13, 2019, date of current version May 24, 2019.

Digital Object Identifier 10.1109/ACCESS.2019.2916391

Electromagnetic Vibration and Noise Comparison of Amorphous Metal PMSMs and Silicon Steel PMSMs

SHENGNAN WU, (Member, IEEE), WENJIE LI, WENMING TONG, (Member, IEEE), AND RENYUAN TANG

National Engineering Research Center for Rare-earth Permanent Magnet Machines, Shenyang University of Technology, Shenyang 110870, China

Corresponding author: Shengnan Wu (imwushengnan@163.com)

This work was supported in part by the National Natural Science Foundation of China under Grant 51677122, and in part by the National Key Research and Development Program of China under Grant 2016YFB0300503.

ABSTRACT This paper investigates the differences in the electromagnetic vibration and noise of an amorphous metal (AM) permanent magnet synchronous machines (PMSMs) and silicon steel (SS) PMSMs. The electromagnetic vibration and noise of an AM PMSM and an SS PMSM sharing the same structure and dimensions are calculated under different conditions: 1) only radial forces (RFs); 2) only magnetostriction (MS) effects; and 3) both RFs and MS effects, and the calculated results of the two machines are compared. The effects of Young's modulus parameters and the MS coefficients of stator cores on the electromagnetic vibration and noise are analyzed. The vibration and noise of the AM PMSM and SS PMSM prototypes are tested and compared with the corresponding calculated results to verify the accuracy of the calculated results.

INDEX TERMS Vibration and noise, permanent magnet synchronous machines (PMSMs), amorphous metal, radial forces, magnetostriction.

I. INTRODUCTION

The smooth and quiet operation performance of permanent magnet synchronous machines (PMSMs) is desired in high performance applications, such as robotics, automobiles, aeronautics and astronautics [1]. The source of vibration and noise in PMSMs can be classified into three categories: aerodynamic, mechanical and electromagnetic. Electromagnetic source is the dominating one in low and medium power rated electrical machines.

Much attentions have been paid to the electromagnetic vibration and noise caused by radial forces (RFs) for electrical machines. In [2], an analytical model has been developed for analyzing the RFs in fractional-slot PMSMs. The analytical model can be used to investigate the influence of the stator slotting, tangential field component, load condition on the RFs calculation. In [3], the electromagnetic vibration and noise in external rotor PMSMs are studied. It is found that the frequency characteristics of RFs acting on surface of permanent magnet is different from that in external stator PMSM. The RFs produced by the interaction of permanent magnet field and stator slotting contributes the most remarkable component to the overall noise. In [4], the global and local force and their effects on vibration in PMSMs are investigated. The local force includes both the tangential forces and RFs distributing on the stator. The main effect of local force is to induce radial vibration of the stator, while global cogging torque and torque ripple may induce remarkable lateral motion. In [5], the electromagnetic vibration in permanent magnet assisted synchronous reluctance machines is studied. It is found that the RFs due to the rotor slot in the flux barriers may cause serious vibration. In [6], [7], the RFs and vibration characteristics of a fault-tolerant flux-switching permanent magnet machine are studied. It is found that the lower order harmonics of RFs have more significant influence than the torque fluctuation on the vibration. In [8], the RFs and electromagnetic vibration in external-rotor switched reluctance motors are studied. It is found that the rotor is a major source of vibration. The effect of switching angles at different vibration modes is analyzed. It is found that the vibration is not uniformly distributed and the displacement on the external-rotor teeth decreases as the modal frequency increases for all

The associate editor coordinating the review of this manuscript and approving it for publication was Qiangqiang Yuan.

positions. In [9], the effect of slotted structure on vibration response in electrical machines is studied. It is found that high spatial order RFs could also induce a low-mode stator vibration with a large amplitude due to the slotting effect, and they could be the main vibration source in the electrical machine. In [10], [11], the electromagnetic vibration and noise in an external-rotor axial-flux motor are studied. It is found that the electromagnetic vibration and noise are excited only when the spatial order of axial electromagnetic force coincides with the circumferential order of modal shapes. In [12]–[18], the influences of current harmonics on the RFs and vibration of electrical machines are studied. Current harmonics are caused by pulse width modulation and nonsinusoidal back electromotive force. RFs harmonics due to current harmonics induce extra vibration and noise. In [19]–[25], the influences of slot/pole combinations on the RFs and vibration of electrical machines are studied. The RFs and vibration are strictly dependent on the slot/pole combinations. In fractional slot electrical machines, the vibration and noise can be significantly higher since the dominant vibration mode order can be as low as 1 or 2.

Magnetostriction (MS) is a property of ferromagnetic material in which the material exhibits strain in the presence of magnetic field and is recognized as another cause of the electromagnetic vibration and noise next to RFs for electrical machines [26]. A common approach to incorporating the effect of magnetostriction on the material is through a set of MS forces. In [27], [28], the MS models employ the principle of virtual work to determine the set of MS forces from the magnetic field. Measured data on magnetization curves under stress levels are used in obtaining the nonlinear transient numerical solutions. The model is implemented on a 2-hp permanent magnet electrical motor. The results show that MS forces are significant and amount to more than 50% force level increase above RFs levels obtained without accounting for MS. In [29]–[31], a model for the simulation of magnetoelastic coupling in electrical machines is studied. The MS forces are calculated and the effect of MS on the vibrational behavior of the stator of electrical machines is obtained. The MS damps the vibrations at some frequencies and increases them at others. The velocities of vibrations at some frequencies are found to be 8 to 9 times larger when the MS is taken into account. In [32]–[34], the MS models employ experimental data from MS elongation to calculate the corresponding set of MS forces through the stress-strain constitutive relations. The stator vibration caused by RFs and MS effect for a 45-kW induction machine is calculated. The results show that the vibrations due to MS are considerably smaller than the effect due to RFs, except for the 100 Hz force component. In [35], [36], a monovalent model and a NN-based model are presented to calculate the vibration due to MS. The effects of RFs and MS on the vibration for induction machine are studied. The results show that the contributions of the RFs and MS to the vibrations of an electrical machine can either add up or subtract, depending on the geometry of the electrical machine and the deformation mode. In [37]–[39], an energy-based magneto-mechanical model for electrical machines is developed and the deformations in an induction machine are investigated. The results show that the contribution of MS and magnetic stress in iron tends to expand the shape of the electrical machine. The effect of the electromagnetic stress is small with respect to the deformations resulting from the MS. RFs into the computation have an enormous influence on the displacements of the stator and the rotor. In [40], [41], the contributions to vibration from RFs and the MS effect for large electrical machines are studied. The results show that MS can act either to reduce or increase the overall modal excitation compared to the excitation of RFs. In [42], the effect of MS on vibration of an interior permanent magnet motor is studied. The results show that the displacement is significantly affected by the MS when the shrink-fit stress is considered. In [43], [44], a strong coupled magneto-elastic model based on piezomagnetic laws is developed to calculate the deformation of the stator for electrical machines. The vibration of a PMSM is analyzed. The results show that the MS effect has significant influence on vibration and it must be considered for design lower vibration and noise motor.

The electromagnetic vibration and noise for different types of silicon steel (SS) electrical machines have been studied extensively. The PMSMs with the stator cores made from amorphous metal (AM) materials are called AM PMSMs. AM materials are non-crystal alloy characterized by extremely low loss and high magnetic permeability. The excellent properties of AM materials offer some possibility to increase PMSM efficiency with AM cores. However, the stiffness and the lamination factor of AM stator cores are low, and the elastic modulus of AM materials is about half of conventional SS materials. Furthermore, the MS coefficient of AM materials is much larger than SS materials. Therefore, the electromagnetic vibration and noise of AM PMSMs are different from SS PMSMs. The vibration and noise of AM PMSMs are rarely studied. This paper investigates the differences in the electromagnetic vibration and noise of AM PMSMs and SS PMSMs. Firstly, the electromagnetic vibration and noise of an AM PMSM and a SS PMSM sharing the same structure and dimensions are calculated under different conditions which are (a) only RFs (b) only MS effects (c) both RFs and MS effects respectively. Furthermore, the effects of Young's modulus parameters and MS coefficients of stator cores on the electromagnetic vibration and noise are analyzed. Lastly, the vibration and noise of the AM PMSM and SS PMSM prototypes are tested to verify the accuracy of the calculated results.

II. SOURCES OF ELECTROMAGNETIC VIBRATION AND NOISE

A. RFs

RFs density distribution on the stator teeth surface, which results from the air-gap magnetic field, is the main cause of electromagnetically induced vibration and noise, and can

be evaluated analytically by Maxwell's stress method [45]. Thus,

$$f_{\text{rad}}(\theta_s, t) = \frac{1}{2\mu_0}\left[B_r^2(\theta_s, t) - B_\theta^2(\theta_s, t)\right] \quad (1)$$

where, f_{rad} is the radial component of forces density (N/m^2), B_r and B_θ are the radial and tangential components of the magnetic flux density in the air-gap, μ_0 is the permeability of free space, θ_s is the angular position at the stator, and t is the time.

Since the magnetic permeability of the ferromagnetic core is much higher than that of the air gap, the magnetic flux lines are practically perpendicular to the stator and rotor cores. This means the tangential component of magnetic flux is much smaller than the radial component and can be neglected. Therefore, the instantaneous value of RFs density is given by

$$f_{\text{rad}}(\theta_s, t) = \frac{B_r^2(\theta_s, t)}{2\mu_0} \quad (2)$$

B. MS EFFECTS

Assuming isotropic and isochoric magnetostriction [46], when magnetic flux density B is along x axis, the MS strain tensor ε_{ms} is given by

$$\varepsilon_{\text{ms}} = \begin{bmatrix} \lambda & -\frac{\lambda}{2} & -\frac{\lambda}{2} & 0 & 0 & 0 \end{bmatrix} \quad (3)$$

where $\lambda = \lambda(B)$ is the magnetostriction strain in the direction of B (x direction).

The system of PMSMs may have both MS and elastic strains. It is obvious that $\varepsilon = \varepsilon_{\text{ms}} + \varepsilon_{\text{elast}}$, where ε is the total strain. Only the elastic strain contributes to mechanical stress [33]. According to Hook's law

$$\sigma = \boldsymbol{D}\varepsilon_{\text{elast}} = \boldsymbol{D}\varepsilon - \boldsymbol{D}\varepsilon_{\text{ms}} \quad (4)$$

where σ is the stress tensor, $\boldsymbol{D}$ is the stiffness tensor, $\varepsilon_{\text{elast}}$ is the elastic strain tensor, and ε_{ms} is MS strain tensor.

Now we define σ_{ms} as the MS stress tensor which is minus the internal stress due to MS.

$$\sigma_{\text{ms}} = -\boldsymbol{D}\varepsilon_{\text{ms}} \quad (5)$$

III. ELECTROMAGNETIC VIBRATION AND NOISE ANALYSIS OF AM PMSMs and SS PMSMs

A. STRUCTURE AND PARAMETERS OF THE AM PMSM AND THE SS PMSM

An AM PMSM and a SS PMSM sharing the same structure and dimensions are studied in this paper. The structures of the two PMSMs are shown in Fig.1, and their parameters are listed in Table 1. The stator core of the AM PMSM is made of 2605SA1, and the stacking factor of the stator core is 0.9. The stator core of the SS PMSM is made of 35W270, and the stacking factor of the stator core is 0.97.

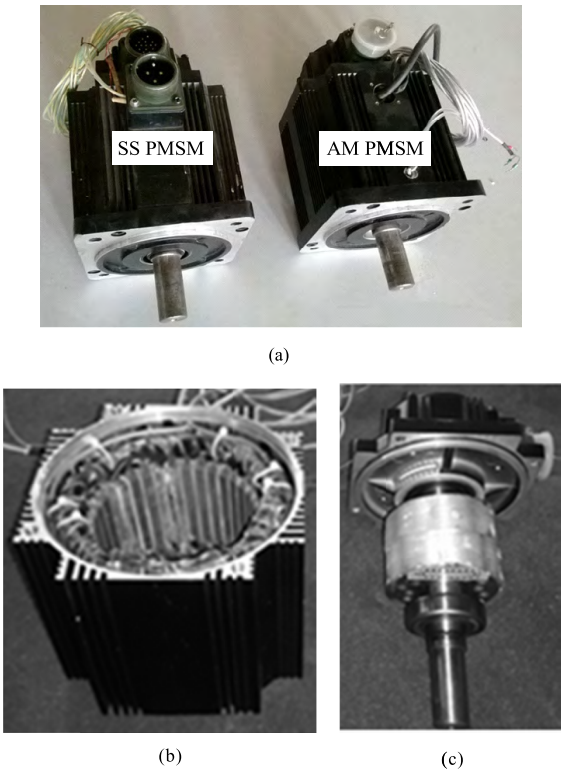

FIGURE 1. Illustration of (a) 2.1kW, 4000 r/min AM PMSM and SS PMSM prototypes (b) stator (c) rotor.

TABLE 1. Parameters of the 2.1kW AM PMSM and SS PMSM Prototypes.

Parameters	Value	Parameters	Value
Rated speed, r·min^{-1}	4000	Air gap length, mm	1.5
Rated frequency, Hz	267	Stator core outer diameter, mm	123
Pole number	8	Stator core inner diameter, mm	81
Stator slots number	36	Axial length, mm	54

B. ELECTROMAGNETIC VIBRATION AND NOISE ANALYSIS

Multi-physics models are established to calculate the electromagnetic vibration and noise of the two PMSMs. The electromagnetic field of the two PMSMs is calculated under rated operating conditions. Fig.2 shows the air-gap flux density

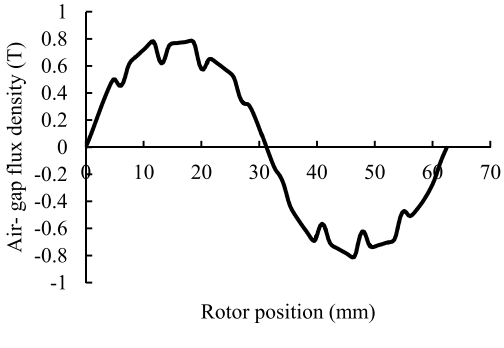

FIGURE 2. Air-gap flux density distributions of the AM PMSM.

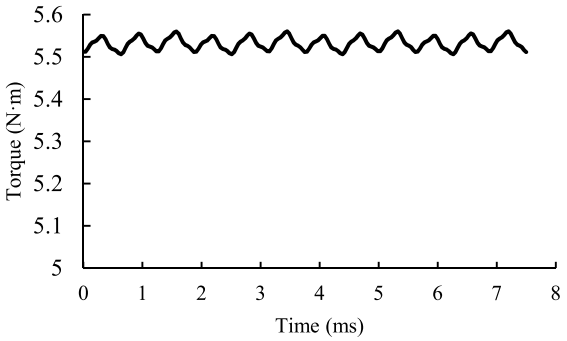

FIGURE 3. Torque waveform of the AM PMSM.

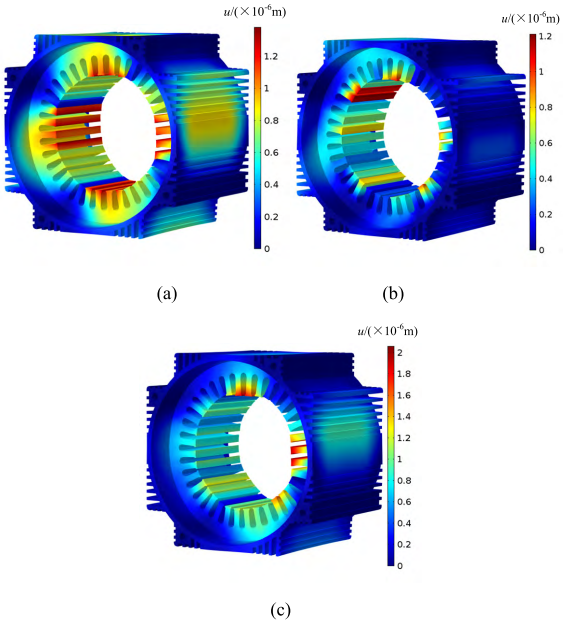

FIGURE 4. Stator and housing deformation of the AM PMSM. (a) Only RFs. (b) Only MS effects. (c) Both RFs and MS effects.

distribution of the AM PMSM. The air-gap flux densities of the AM PMSM and SS PMSM are almost identical. Fig.3 shows the torque waveform of the AM PMSM. The AM PMSM and SS PMSM have the almost same output torque and torque ripple. The average torque of the AM PMSM is 5.53N·m and the peak-to-peak torque ripple is about 0.05N·m. The vibration deformations of the two PMSMs are analyzed under different conditions (a) only RFs (b) only MS effects (c) both RFs and MS effects respectively. Fig.4 and 5 show the stator and housing deformations of the AM PMSM and SS PMSM, respectively. It can be seen from the figures that the stator and housing deformation distributions of the AM PMSM and SS PMSM are almost the same, but the deflection value of the AM PMSM is significantly larger than that of the SS PMSM.

Electromagnetic vibration accelerations of the two PMSMs are calculated when they operate under different working

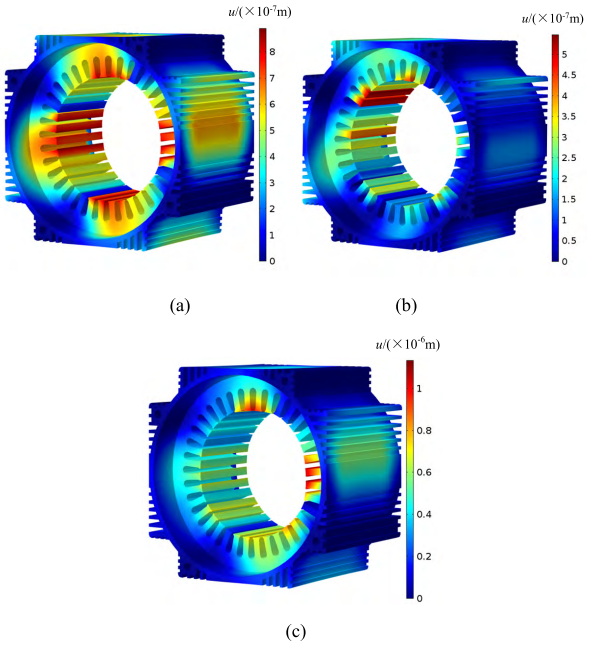

FIGURE 5. Stator and housing deformations of the SS PMSM. (a) Only RFs. (b) Only MS effects. (c) Both RFs and MS effects.

TABLE 2. Calculated results of the electromagnetic vibration acceleration of the AM PMSM under different working speeds.

Speed, r·min^{-1}	Vibration acceleration, m·s^{-2}			Vibration with MS effects is increased by percentage k_1, %
	RFs	MS effects	RFs and MS effects	
1000	0.176	0.060	0.188	6.8
2000	0.719	0.255	0.770	7.1
3000	1.57	0.552	1.69	7.6
4000	3.01	1.04	3.25	8.0

TABLE 3. Calculated results of the electromagnetic vibration acceleration of the SS PMSM under different working speeds.

Speed, r·min^{-1}	Vibration acceleration, m·s^{-2}			Vibration with MS effects is increased by percentage k_2, %
	RFs	MS effects	RFs and MS effects	
1000	0.091	0.042	0.097	6.6
2000	0.369	0.178	0.394	6.8
3000	0.802	0.393	0.855	6.6
4000	1.52	0.746	1.63	7.2

speeds, and the calculated results are shown in Table 2 and Table 3. It can be concluded that, on average, the electromagnetic vibration with MS effects is increased by 7.4% in the AM PMSM, and the vibration with MS effects is increased by 6.8% in the SS PMSM. Table 4 and Table 5 show electromagnetic noise of the two PMSMs under different working speeds, respectively. It can be concluded that, on average, the electromagnetic noise with MS effects is increased by 1.2% in the AM PMSM, and the noise with MS effects is increased by 1.2% in the SS PMSM.

TABLE 4. Calculated results of the electromagnetic noise of the AM PMSM under different working speeds.

Speed, r·min^{-1}	Average sound pressure level, dB(A)		Noise with MS effects is increased by percentage k_3, %
	RFs	RFs and MS effects	
1000	54.3	55.0	1.3
2000	59.9	60.6	1.2
3000	62.4	63.2	1.3
4000	64.9	65.7	1.2

TABLE 5. Calculated results of the electromagnetic noise of the SS PMSM under different working speeds.

Speed, r·min^{-1}	Average sound pressure level, dB(A)		Noise with MS effects is increased by percentage k_4, %
	RFs	RFs and MS effects	
1000	49.0	49.6	1.2
2000	54.5	55.1	1.1
3000	57.1	57.8	1.2
4000	59.5	60.2	1.2

C. COMPARISONS OF ELECTROMAGNETIC VIBRATION AND NOISE FOR THE AM PMSMs and SS PMSMs

Table 6 and Table 7 show the comparisons of the electromagnetic vibration acceleration and noise for the two PMSMs under different working speeds. It can be concluded that, on average, the electromagnetic vibration acceleration of the AM PMSM is 1.10 times larger than that of the SS PMSM, and the electromagnetic noise of the AM PMSM is 11% (6.2dB(A)) higher than that of the SS PMSM.

TABLE 6. Comparisons of the electromagnetic vibration acceleration for the AM PMSM and SS PMSM.

Speed, r·min^{-1}	Vibration acceleration, m·s^{-2}		Increased multiplier of vibration of AM PMSM over that of SS PMSM k_5
	AM PMSM	SS PMSM	
1000	0.204	0.099	1.06
2000	0.835	0.402	1.08
3000	1.85	0.875	1.11
4000	3.55	1.67	1.13

TABLE 7. Comparisons of the electromagnetic noise for the AM PMSM and SS PMSM.

Speed, r·min^{-1}	Average sound pressure level, dB(A)		Increased percentage of noise of AM PMSM over that of SS PMSM k_6, %
	AM PMSM	SS PMSM	
1000	55.9	49.8	12.2
2000	61.5	55.4	11.0
3000	64.3	58.1	10.7
4000	66.7	60.5	10.2

IV. EFFECTS OF YOUNG'S MODULUS ON ELECTROMAGNETIC VIBRATION AND NOISE

Young's modulus of different materials vary widely, for instance, the Young's modulus of conventional SS sheet is 2.06×10^{11}N/m^2, while the Young's modulus of AM strip is only 1.1×10^{11}N/m^2. The effects of Young's modulus parameters of stator cores on the electromagnetic vibration and noise are analyzed, and the calculated results are show in Table 8, Table 9 and Fig.6. It can be concluded that the electromagnetic vibration due to RFs is inversely proportional to the Young's modulus parameters of stator cores, and the Young's modulus parameters of stator cores have little impact on the vibration and noise due to MS effects. When Young's modulus parameters of stator cores vary in the range of $0.5 - 2.0 \times 10^{11}$N/m^2, electrical machine vibration with MS effects increases by 2.5-20.4% and noise with MS effects increases by 0.3-2.7%, 0.4-1.6dB(A). With the increase of Young modulus parameters of stator cores, the effect of MS on electrical machine vibration and noise become larger.

TABLE 8. Effects of Young's modulus parameters of stator cores on the electromagnetic vibration.

Young's modulus $\times 10^{11}$N·m^{-2}	Vibration acceleration, m·s^{-2}			Vibration with MS effects is increased by percentage k_7, %
	RFs	MS effects	RFs and MS effects	
0.5	7.01	1.05	7.19	2.5
1.0	3.30	1.04	3.54	7.4
1.5	2.15	1.04	2.47	14.9
2.0	1.62	1.02	1.95	20.4

TABLE 9. Effects of Young's modulus parameters of stator cores on the electromagnetic noise.

Young's modulus , $\times 10^{11}$N·m^{-2}	Average sound pressure level, dB(A)		Noise with MS effects is increased by percentage k_8, %
	RFs	RFs and MS effects	
0.5	72.6	72.8	0.3
1.0	66.1	66.7	0.9
1.5	62.5	63.7	1.9
2.0	60.0	61.6	2.7

TABLE 10. Decreased multiplier of electromagnetic vibration and noise with different Young's modulus parameters of stator cores.

Decreased multiplier of electromagnetic vibration and noise	Variation range of Young's modulus parameters of stator cores		
	$k_{E=1.0/E=0.5\times10^{11}\ \mathrm{N\cdot m^{-2}}}$	$k_{E=1.5/E=1.0\times10^{11}\ \mathrm{N\cdot m^{-2}}}$	$k_{E=2.0/E=1.5\times10^{11}\ \mathrm{N\cdot m^{-2}}}$
Vibration k_9, %	50.7	30.3	21.1
Noise k_{10}, %	8.4	4.5	3.3
Noise, dB(A)	6.1	3.0	2.1

Table 10 shows decreased multiplier of electromagnetic vibration and noise of electrical machines with different Young's modulus parameters of stator cores. It can be concluded that with the increase of Young's modulus parameters of stator cores, the decreased multiplier of electromagnetic vibration and noise becomes smaller. When Young's modulus parameters are in the range of $0.5\text{-}2.0\times10^{11}$N/m^2, the electromagnetic vibration of electrical machines decreases by 21.1-50.7% and electromagnetic noise decreases by 3.3-8.4%, 2.1-6.1dB(A) with the increase of Young's modulus by 0.5×10^{11}N/m^2.

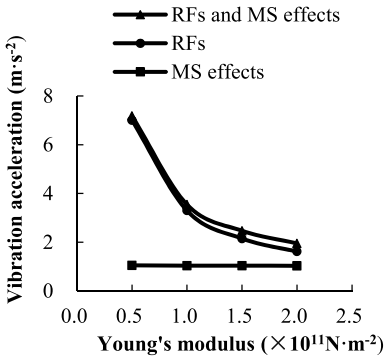

(a)

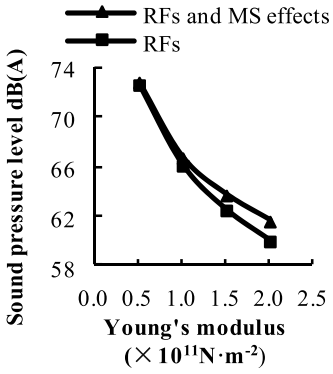

(b)

FIGURE 6. Electromagnetic vibration and noise versus Young's modulus parameters of stator cores. (a) Vibration. (b) Noise.

V. EFFECTS OF MS COEFFICIENTS ON ELECTROMAGNETIC VIBRATION AND NOISE

MS coefficients of different materials vary widely, for instance, the MS coefficient of non-oriented SS sheet is 9.204×10^{-6}, while the MS coefficient of AM 2605SA1 is up to 26×10^{-6}. The effects of MS coefficients of stator cores on the electromagnetic vibration and noise are analyzed, and the calculated results are show in Table 11, Table 12 and Fig.7. It can be concluded that the electromagnetic vibration due to MS effects is proportional to the MS coefficients of stator cores. When MS coefficients of stator cores vary in the range of $10 - 40 \times 10^{-6}$, electrical machine vibration with MS effects increases by 2.3-16.3% and noise with MS effects increases by 0.5-2.2%, 0.3-1.4dB(A). With the increase of MS coefficients of stator cores, the effects of MS effects on electrical machine vibration and noise become larger.

Table 13 shows increased multiplier of electromagnetic vibration and noise of electrical machines with different MS coefficients of stator cores. It can be concluded that with the increase of MS coefficients of stator cores, the decreased multiplier of vibration and noise becomes larger. When MS coefficients are in the range of $10-40\times10^{-6}$, the electromagnetic vibration increases by 3.2-6.4% and electromagnetic noise increases by 0.3-0.9%, 0.2-0.6 dB(A) with the increase of MS coefficients by 10×10^{-6}.

TABLE 11. Effects of MS coefficients of stator cores on the electromagnetic vibration.

MS coefficients, $\times10^{-6}$	Vibration acceleration, $m\cdot s^{-2}$			Vibration with MS effects is increased by percentage k_{11}, %
	RFs	MS effects	RFs and MS effects	
10	3.01	0.386	3.08	2.3
20	3.01	0.774	3.18	5.6
30	3.01	1.16	3.29	9.3
40	3.01	1.55	3.50	16.3

TABLE 12. Effects of MS coefficients of stator cores on the electromagnetic noise.

MS coefficients, $\times10^{-6}$	Average sound pressure level, dB(A)		Noise with MS effects is increased by percentage k_{12}, %
	RFs	RFs and MS effects	
10	64.9	65.2	0.5
20	64.9	65.4	0.8
30	64.9	65.7	1.2
40	64.9	66.3	2.2

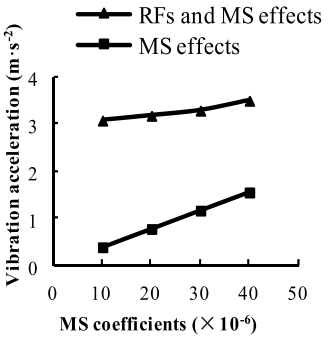

(a)

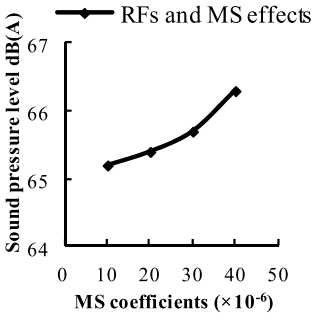

(b)

FIGURE 7. Electromagnetic vibration and noise versus MS coefficients of stator cores. (a) Vibration. (b) Noise.

VI. EXPERIMENTS INVESTIGATIONS

The AM PMSM and SS PMSM prototypes are manufactured. An experiment platform is built to measure the vibration and noise of the two prototypes. The prototypes are placed in the anechoic chamber, and the noise test circumstance is shown

TABLE 13. Increased multiplier of electromagnetic vibration and noise with different MS coefficients of stator cores.

Increased multiplier of electromagnetic vibration and noise	Variation range of MS coefficients of stator cores		
	$k_{\lambda=20/\lambda=10\times10^{-6}}$	$k_{\lambda=30/\lambda=20\times10^{-6}}$	$k_{\lambda=40/\lambda=30\times10^{-6}}$
Vibration k_{13}, %	3.2	3.5	6.4
Noise k_{14}, %	0.3	0.5	0.9
Noise, dB(A)	0.2	0.3	0.6

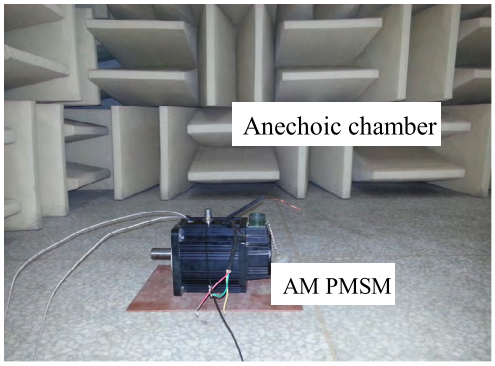

(a)

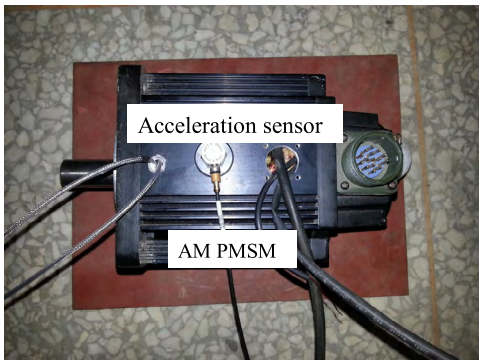

(b)

FIGURE 8. Experiment platform. (a) Noise test circumstance. (b) Vibration acceleration test point.

TABLE 14. Comparisons between calculated data and experimental data of noise for the AM PMSM under different working speeds.

Speed, r·min^{-1}	Average sound pressure level, dB(A)		Relative error, %
	Calculated data	Experimental data	
1000	55.9	60.1	7.0
2000	61.5	63.9	3.8
3000	64.3	66.4	3.2
4000	66.7	68.5	2.6

in Fig.8a. The position of microphones Noise test points are arranged in the front, back left and right directions of the prototype. The radius of the test points is 0.4m and the height of the test points is 0.25m. Acceleration sensors are attached to prototypes to measure the vibration acceleration as shown in Fig.8b. The flow chart of vibration and noise measurement system is shown in Fig.9.

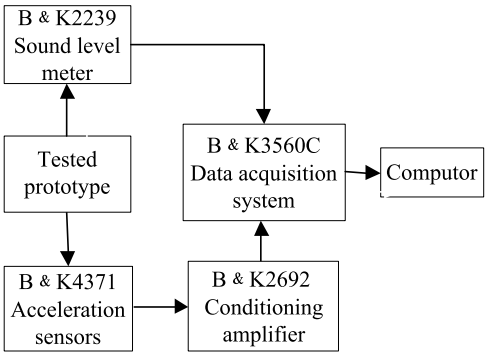

FIGURE 9. Flow chart of vibration and noise measurement system.

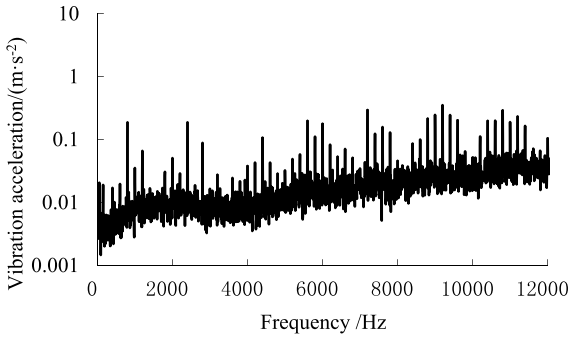

FIGURE 10. Frequency domain waveform of vibration acceleration for the AM PMSM at rated speed.

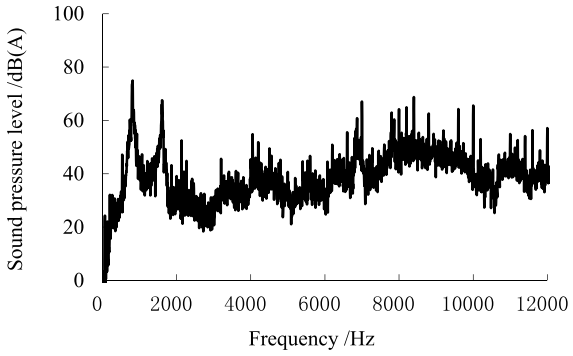

FIGURE 11. Frequency domain waveform of noise for the AM PMSM at rated speed.

The vibration acceleration and sound pressure level of the two prototypes are tested under different working speeds. Fig.10 shows the frequency domain waveform of vibration acceleration for the AM PMSM at rated speed. Fig.11 shows the frequency domain waveform of sound pressure level for the AM PMSM at rated speed. Calculated results are compared with the experimental results. Table 14 and Table 15 show the comparisons between calculated results and experimental results of the noise for the AM PMSM and SS PMSM, respectively. The comparisons show that the

TABLE 15. Comparisons between calculated and experimental data of noise for the SS PMSM under different working speeds.

Speed, $r \cdot min^{-1}$	Average sound pressure level, dB(A)		Relative error, %
	Calculated data	Experimental data	
1000	49.8	54.7	8.9
2000	55.4	58.3	5.0
3000	58.1	59.8	2.8
4000	60.5	61.6	1.8

maximum relative error of the noise for the AM PMSM is 7.0% and that for the SS PMSM is 8.9%. Experimental results demonstrate that the calculation method is feasible.

VII. CONCLUSION

In this paper, the differences in the electromagnetic vibration and noise of AM PMSMs and SS PMSMs are studied, and some conclusions are obtained. The electromagnetic vibration and noise with MS effects is increased by 7.4% and 1.2% in the AM PMSM. The electromagnetic vibration and noise with MS effects is increased by 6.8% and 1.2% in the SS PMSM. The electromagnetic vibration of the AM PMSM is 1.10 times larger than that of the SS PMSM, and the electromagnetic noise of the AM PMSM is 11% (6.2dB(A)) higher than that of the SS PMSM. The electromagnetic vibration due to RFs is inversely proportional to the Young's modulus parameters of stator cores. The electromagnetic vibration due to MS effects is proportional to the MS coefficients of the stator cores.

REFERENCES

[1] R. Islam and I. Husain, "Analytical model for predicting noise and vibration in permanent-magnet synchronous motors," *IEEE Trans. Ind. Appl.*, vol. 46, no. 6, pp. 2346–2354, Nov./Dec. 2010.

[2] Z. Q. Zhu, Z. P. Xia, L. J. Wu, and G. W. Jewell, "Analytical modeling and finite-element computation of radial vibration force in fractional-slot permanent-magnet brushless machines," *IEEE Trans. Ind. Appl.*, vol. 46, no. 5, pp. 1908–1918, Sep./Oct. 2010.

[3] S. Zuo, F. Lin, and X. Wu, "Noise analysis, calculation, and reduction of external rotor permanent-magnet synchronous motor," *IEEE Trans. Ind. Elect.*, vol. 62, no. 10, pp. 6204–6212, Oct. 2015.

[4] J. Zou, H. Lan, Y. Xu, and B. Zhao, "Analysis of global and local force harmonics and their effects on vibration in permanent magnet synchronous machines," *IEEE Trans. Energy Convers.*, vol. 32, no. 4, pp. 1523–1532, Dec. 2017.

[5] Y. Lu *et al.*, "Electromagnetic force and vibration analysis of permanent-magnet-assisted synchronous reluctance machines," *IEEE Trans. Ind. Appl.*, vol. 54, no. 5, pp. 4246–4256, Sep./Oct. 2018.

[6] Y. Mao, G. Liu, W. Zhao, and J. Ji, "Vibration prediction in fault-tolerant flux-switching permanent-magnet machine under healthy and faulty conditions," *IET Electr. Power Appl.*, vol. 11, no. 1, pp. 19–28, Jan. 2017.

[7] Y. Mao, G. Liu, W. Zhao, J. Ji, and Z. Wang, "Low-noise design of fault-tolerant flux-switching permanent-magnet machines," *IET Electr. Power Appl.*, vol. 12, no. 6, pp. 747–756, Jul. 2018.

[8] S. M. Castano, B. Bilgin, J. Lin, and A. Emadi, "Radial forces and vibration analysis in an external-rotor switched reluctance machine," *IET Electr. Power Appl.*, vol. 11, no. 2, pp. 252–259, Mar. 2017.

[9] H. Fang, D. Li, R. Qu, and P. Yan, "Modulation effect of slotted structure on vibration response in electrical machines," *IEEE Trans. Ind. Electron.*, vol. 66, no. 4, pp. 2998–3007, Apr. 2019.

[10] W. Deng, S. Zuo, F. Lin, and S. Wu, "Influence of pole and slot combinations on vibration and noise in external rotor axial flux in-wheel motors," *IET Electr. Power Appl.*, vol. 11, no. 4, pp. 586–594, Apr. 2017.

[11] W. Deng and S. Zuo, "Analytical modeling of the electromagnetic vibration and noise for an external-rotor axial-flux in-wheel motor," *IEEE Trans. Ind. Electron.*, vol. 65, no. 3, pp. 1991–2000, Mar. 2018.

[12] D. Torregrossa, D. Paire, F. Peyraut, B. Fahimi, and A. Miraoui, "Active mitigation of electromagnetic vibration radiated by PMSM in fractional-horsepower drives by optimal choice of the carrier frequency," *IEEE Trans. Ind. Electron.*, vol. 59, no. 3, pp. 1346–1354, Mar. 2012.

[13] I. P. Tsoumas and H. Tischmacher, "Influence of the inverter's modulation technique on the audible noise of electric motors," *IEEE Trans. Ind. Appl.*, vol. 50, no. 1, pp. 269–278, Jan./Feb. 2014.

[14] F. Lin, S. Zuo, W. Deng, and S. Wu, "Modeling and analysis of electromagnetic force, vibration, and noise in permanent-magnet synchronous motor considering current harmonics," *IEEE Trans. Ind. Electron*, vol. 63, no. 12, pp. 7455–7466, Dec. 2016.

[15] W. Liang, P. C. Luk, and W. Fei, "Analytical investigation of sideband electromagnetic vibration in integral-slot PMSM drive with SVPWM technique," *IEEE Trans. Power Electron.*, vol. 32, no. 6, pp. 4785–4795, Jun. 2017.

[16] X. Guo, R. Zhong, L. Zhao, J. Yin, and W. Sun, "Method for radial vibration modelling in switched reluctance motor," *IET Electr. Power Appl.*, vol. 10, no. 9, pp. 834–842, Nov. 2016.

[17] X. Guo, R. Zhong, D. Ding, M. Zhang, W. Shao, and W. Sun, "Origin of resonance noise and analysis of randomising turn-on angle method in switched reluctance motor," *IET Electr. Power Appl.*, vol. 11, no. 7, pp. 1324–1332, Aug. 2017.

[18] R. Zhong, X. Guo, M. Zhang, D. Ding, and W. Sun, "Influence of switch angles on second-order current harmonic and resonance in switched reluctance motors," *IET Electr. Power Appl.*, vol. 12, no. 9, pp. 1247–1255, Nov. 2018.

[19] Z. Q. Zhu, Z. P. Xia, L. J. Wu, and G. W. Jewell, "Influence of slot and pole number combination on radial force and vibration modes in fractional slot PM brushless machines having single- and double-layer windings," in *Proc. IEEE Energy Convers. Cong. Expo.*, Sep. 2009, pp. 3443–3450.

[20] J. Krotsch and B. Piepenbreier, "Radial forces in external rotor permanent magnet synchronous motors with non-overlapping windings," *IEEE Trans. Ind. Appl.*, vol. 59, no. 5, pp. 2267–2276, May 2012.

[21] G. Verez, G. Barakat, Y. Amara, and G. Hoblos, "Impact of pole and slot combination on vibrations and noise of electromagnetic origins in permanent magnet synchronous motors," *IEEE Trans. Magn.*, vol. 51, no. 3, Mar. 2015, Art. no. 8101104.

[22] D.-Y. Kim, M.-P. Park, J.-H. Sim, and J.-P. Hong, "Advanced method of selecting number of poles and slots for low-frequency vibration reduction of traction motor for elevator," *IEEE/ASME Trans. Mechatronics*, vol. 22, no. 4, pp. 1554–1562, Aug. 2017.

[23] F. Lin, S. Zuo, and X. Wu, "Electromagnetic vibration and noise analysis of permanent magnet synchronous motor with different slot-pole combinations," *IET Electr. Power Appl.*, vol. 10, no. 9, pp. 900–908, Nov. 2016.

[24] E. Carraro, N. Bianchi, S. Zhang, and M. Koch, "Design and performance comparison of fractional slot concentrated winding spoke type synchronous motors with different slot-pole combinations," *IEEE Trans. Ind. Appl.*, vol. 54, no. 3, pp. 2276–2284, May/Jun. 2018.

[25] M. Qiao, C. Jiang, y. Zhu, and G. Li, "Research on design method and electromagnetic vibration of six-phase fractional-slot concentrated-winding PM motor suitable for ship propulsion," *IEEE Access*, vol. 4, pp. 8535–8543, 2016.

[26] P. I. Anderson, A. J. Moses, and H. J. Stanbury, "Assessment of the stress sensitivity of magnetostriction in grain-oriented silicon steel," *IEEE Trans. Magn.*, vol. 43, no. 8, pp. 3467–3476, Aug. 2007.

[27] O. A. Mohammed, T. Calvert, and R. McConnell, "A model for magnetostriction in coupled nonlinear finite element magneto-elastic problems in electrical machines," in *Proc. IEEE Int. Conf. Elect. Mach. Drives*, May 1999, pp. 728–735.

[28] O. A. Mohammed, T. Calvert, and R. McConnell, "Coupled magnetoelastic finite element formulation including anisotropic reluctivity tensor and magnetostriction effects for machinery applications," *IEEE Trans. Magn.*, vol. 37, no. 5, pp. 3388–3392, Sep. 2001.

[29] A. Belahcen, "Magnetoelestticity, magnetic forces and magnetostriction in electrical machines," Ph.D. dissertation, Dept. Electr. Commun. Eng., Helsinki Univ. Technol., Espoo, Finland, 2004.

[30] A. Belahcen, "Magnetoelastic coupling in rotating electrical machines," *IEEE Trans. Magn.*, vol. 41, no. 5, pp. 1624–1627, May 2005.

[31] A. Belahcen, "Vibrations of rotating electrical machines due to magnetomechanical coupling and magnetostriction," *IEEE Trans. Magn.*, vol. 42, no. 4, pp. 971–974, Apr. 2006.

[32] K. Delaere, W. Heylen, K. Hameyer, and R. Belmans, "Local magnetostriction forces for finite element analysis," *IEEE Trans. Magn.*, vol. 36, no. 5, pp. 3115–3118, Sep. 2000.
[33] K. Delaere, W. Heylen, R. Belmans, and K. Hameyer, "Comparison of induction machine stator vibration spectra induced by reluctance forces and magnetostriction," *IEEE Trans. Magn.*, vol. 38, no. 2, pp. 969–972, Mar. 2002.
[34] K. Delaere, "Computation and experimental analysis of electrical machine vibrations caused by magnetic forces and magnetostriction," Ph.D. dissertation, ESAT, Katholieke Univ., Leuven, Belgium, 2004.
[35] T. Hilgert, L. Vandevelde, and J. Melkebeek, "Comparison of magnetostriction models for use in calculations of vibrations in magnetic cores," *IEEE Trans. Magn.*, vol. 44, no. 6, pp. 874–877, Jun. 2008.
[36] T. G. D. Hilgert, L. Vandevelde, and J. A. A. Melkebeek, "Numerical analysis of the contribution of magnetic forces and magnetostriction to the vibrations in induction machines," *IET Sci., Meas. Technol.*, vol. 1, no. 1, pp. 21–24, Jan. 2007.
[37] K. A. Fonteyn, "Energy-based magneto-mechanical model for electrical steel sheets," Ph.D. dissertation, Dept. Elect. Eng., Aalto Univ. Espoo, Finland, 2010.
[38] K. Fonteyn, A. Belahcen, R. Kouhia, P. Rasilo, and A. Arkkio, "FEM for directly coupled magneto-mechanical phenomena in electrical machines," *IEEE Trans. Magn.*, vol. 46, no. 8, pp. 2923–2926, Aug. 2010.
[39] K. A. Fonteyn, A. Belahcen, P. Rasilo, R. Kouhia, and A. Arkkio, "Contribution of Maxwell stress in air on the deformations of induction machines," in *Proc. Int. Conf. Elect. Mach. Syst.*, vol. 1, Oct. 2010, 1749-1753.
[40] A. Shahaj, "Mitigation of vibration in large electrical machines," Ph.D. dissertation, School Mech., Mater. Manuf. Eng., Univ. Nottingham, Nottingham, U.K., 2010.
[41] A. Shahaj and S. D. Garvey, "A possible method for magnetostrictive reduction of vibration in large electrical machines," *IEEE Trans. Magn.*, vol. 47, no. 2, pp. 374–385, Feb. 2011.
[42] H. Ebrahimi, Y. Gao, H. Dozono, K. Muramatsu, T. Okitsu, and D. Matsuhashi, "Effects of stress and magnetostriction on loss and vibration characteristics of motor," *IEEE Trans. Magn.*, vol. 52, no. 3, Mar. 2016, Art. no. 8201404.
[43] L. Zhu, Q. Yang, R. Yan, Y. Li, and W. Yan, "Magnetoelastic numerical analysis of permanent magnet synchronous motor including magnetostriction effects and harmonics," *IEEE Trans. Appl. Supercond.*, vol. 24, no. 3, Jun. 2014, Art. no. 0503304.
[44] L. Zhu, B. Wang, R. Yan, Q. Yang, Y. Yang, and X. Zhang, "Electromagnetic vibration of motor core including magnetostriction under different rotation speeds," *IEEE Trans. Magn.*, vol. 52, no. 3, Mar. 2016, Art. no. 8102004.
[45] G. Dajaku and D. Gerling, "Magnetic radial force density of the PM machine with 12-teeth/10-poles winding topology," in *Proc. IEEE Int. Electr. Mach. Drives Conf.*, May 2009, pp. 1715–1720.
[46] H. Ebrahimi, Y. Gao, A. Kameari, H. Dozono, and K. Muramatsu, "Coupled magneto-mechanical analysis considering permeability variation by stress due to both magnetostriction and electromagnetism," *IEEE Trans. Magn.*, vol. 49, no. 5, pp. 1621–1624, May 2013.

SHENGNAN WU (M'18) was born in Yingkou, China. She received the B.S., M.S., and Ph.D. degrees in electrical engineering from the Shenyang University of Technology, Shenyang, China, in 2008, 2011, and 2017, respectively, where she is currently a Postdoctoral Research Assistant in electrical engineering. Her research interests include electromagnetic design of permanent magnet machines, and vibration and noise of permanent magnet machines.

WENJIE LI was born in Shanxi, China. He received the B.S. in electrical engineering from the Taiyuan University of Technology, Taiyuan, China, in 2016. He is currently pursuing the M.S. degree in electrical engineering with the Shenyang University of Technology.

His research interests include multi-physical field simulation and analysis of permanent magnet machines.

WENMING TONG (M'18) was born in Dandong, China. He received the B.S. and Ph.D. degrees in electrical engineering from the Shenyang University of Technology, Shenyang, China, in 2007 and 2012, respectively, where he is currently an Associate Professor with the National Engineering Research Center for Rare Earth Permanent Magnet Machines. His research interests include the modeling, design, analysis and control of high-speed and low-speed direct-drive permanent magnet machines, axial flux permanent magnet machines, hybrid excitation machines, and high performance machines with new types of soft magnetic materials.

RENYUAN TANG was born in Shanghai, China, in 1931. He received the B.S. degree in electrical engineering from Shanghai Jiaotong University, Shanghai, China, in 1952.

He is currently an Academician with the Chinese Academy of Engineering, a Professor with the Shenyang University of Technology, and the Director of the National Engineering Research Center for Rare-Earth Permanent Magnet Machines. Since 1978, he has been with the Shenyang University of Technology. His current research interests include the design, analysis, and control of rare-earth permanent magnet machines. He has published eight books by his chief editor and translator, and over 133 technical papers. He is recognized as the pioneer and the founder of the China's rare-earth permanent magnet machines.